First investigation and absolute calibration of clumped isotopes in N_2O by mid-IR laser spectroscopy

Kristýna Kantnerová[1,2], Longfei Yu[1], Daniel Zindel[3], Mark S. Zahniser [4], David D. Nelson[4], Béla Tuszon[1], Mayuko Nakagawa[5], Sakae Toyoda[6], Naohiro Yoshida[5,6], Lukas Emmenegger[1], Stefano M. Bernasconi[2], Joachim Mohn[1,*]

[1] Empa, Laboratory for Air Pollution / Environmental Technology, Dübendorf, 8600, Switzerland
[2] ETH Zürich, Department of Earth Sciences, Zürich, 8092, Switzerland
[3] ETH Zurich, Laboratory of Physical Chemistry, Zürich, 8093, Switzerland
[4] Aerodyne Research, Inc., Center for Atmospheric and Environmental Chemistry, Billerica, Massachusetts, 01821, United States
[5] Tokyo Institute of Technology, Earth-Life Science Institute (ELSI), Tokyo, 152-8550, Japan
[6] Tokyo Institute of Technology, Department of Chemical Science and Engineering, School of Materials and Chemical Technology, Yokohama, 226-8503, Japan

*joachim.mohn@empa.ch, Tel. +41 58 765 4687, Fax +41 58 765 1122

ABSTRACT

Rationale: Unravelling the biogeochemical cycle of the potent greenhouse gas nitrous oxide (N_2O) is an underdetermined problem in environmental sciences due to the multiple involved source and sink processes, which complicates mitigation of its emissions. Measuring the doubly isotopically substituted molecules (isotopocules) of nitrous oxide can add new opportunities to fingerprint and constrain its cycle.

Methods: We present a laser spectroscopic technique to selectively and simultaneously measure the eight most abundant isotopocules of N_2O, including three doubly substituted species – so called "clumped isotopes". For the absolute quantification of individual isotopocule abundances, we propose a new calibration scheme that combines thermal equilibration of a working standard gas with a direct mole fraction-based approach.

Results: This method is validated for a large range of isotopic composition values by comparison with other established methods (laser spectroscopy using conventional isotopic scale and isotope-ratio mass spectrometry). Direct intercomparison with recently developed ultra high-resolution mass spectrometry shows clearly advantages of the new laser technique, especially with respect to site specificity of isotopic substitution in the N_2O molecule.

Conclusions: Our study represents a new methodological basis for the measurements of both singly substituted and clumped N_2O isotopes. It bears a high potential to stimulate future research in the N_2O community by establishing a new class of reservoir-insensitive tracers and molecular-scale insights.

INTRODUCTION

Nitrous oxide (N_2O) is an important greenhouse gas (GHG) and potent ozone-depleting substance, leading to the thinning of the ozone layer. It contributes to human-induced global warming by up to 6 %,[1] and is currently the major substance responsible for the depletion of stratospheric ozone.[2] The mixing ratio of N_2O in the atmosphere has increased from a preindustrial value of 270 nmol mol^{-1} before the year 1750 to (331.1 ± 0.1) nmol mol^{-1} in 2018.[3] Anthropogenic activities, primarily the use of fertilizers in agriculture, substantially increase global N_2O emissions at an even faster rate than

previously estimated by the IPCC emission factor approach.[4] In order to mitigate emissions of this long-lived GHG and reduce the thinning of the ozone layer, its global budget, sinks, and sources need to be well characterized. However, the major sources of N_2O, such as ocean, soil, use of fertilizers, or biomass burning, exhibit high spatial and temporal variability that are insufficiently constrained. Despite many extensive studies, mitigation of N_2O emissions remains a great challenge.

Stable isotopic composition of GHGs is a useful proxy for investigating their sources and sinks.[5] N_2O is a linear asymmetric molecule with three distinct sites for isotopic substitution, i.e. the central (α) and terminal (β) nitrogen (N) atoms, and the oxygen (O) atom. Substitution of ^{14}N and ^{16}O by their heavy isotopes ^{15}N and ^{17}O or ^{18}O, respectively, yields in total 12 isotopically substituted molecules or "isotopocules". Isotopocule is a collective term of more frequently used terms isotopologue (isotopic analogue) and isotopomer (isotopic isomer).[6] In this article, the HITRAN[7] notation as specified in Supplementary Table 1, e.g. 446 for the isotopocule $^{14}N^{14}N^{16}O$, is used to represent isotopocule designations.

Usually, the distribution of isotopic species in a sample is reported in the δ notation:

$$\delta X = \frac{R_{sample}}{R_{ref}} - 1 \tag{1}$$

where X denotes ^{15}N, ^{18}O, $^{15}N^{\alpha}$ (for the isotopocule 456), $^{15}N^{\beta}$ (546), 458, etc., and R is the ratio of the abundance of a rare and the most abundant isotopic species 446 for a sample and a reference gas.[8] The international isotope ratio scales of nitrogen and oxygen are referred to atmospheric N_2 (Air-N_2) and Vienna Standard Mean Ocean Water (VSMOW), respectively, with defined primary reference materials and second scale anchors.[9]

The average ^{15}N content in the N_2O molecule ($\delta^{15}N^{bulk} = (\delta^{15}N^{\alpha} + \delta^{15}N^{\beta})/2$) often carries information of nitrogen substrates and reaction kinetics,[10,11] while $\delta^{18}O$ and $\delta^{17}O$ values are applied e.g. for determining substrate sources.[12,13] Moreover, the covalent bonds between $N^{\beta}-N^{\alpha}$ and $N^{\alpha}-O$ are distinct in terms of electron distribution and bond strength, which generally makes ^{15}N substitution favorable at the α position.[14] The resulting difference in abundances between isotopocules 456 and 546, expressed as $\delta^{15}N^{\alpha} - \delta^{15}N^{\beta}$, is denoted as site preference (SP)[15] and comprises valuable information on biogeochemical reaction pathways, as SP values are independent of the ^{15}N isotopic composition of the reaction substrates. Similarly, SP^{17} and SP^{18} are defined as $\delta457 - \delta547$ and $\delta458 - \delta548$, respectively.[16] In the past decades, the δ values have been used as fingerprints to disentangle production and destruction pathways of N_2O, but they have shown limitations with resolving multiple dimensions of the processes involved.[17]

It has been suggested that multiply substituted isotopocules, so called "clumped isotopes", can provide additional constraints for distinguishing the biogeochemical processes cycling N_2O. Generally, clumping of heavy isotopes in a molecule is thermodynamically favored in an equilibrium process as bonds between heavier isotopes are more stable.[18] Since the extent of clumping is temperature-dependent for equilibrium processes, the abundance of clumped isotopes reflects the formation temperature for the products.[19] This approach has been used mainly in carbonate paleothermometry to study palaeoclimatic and geological processes on Earth.[20] Similarly, N_2O clumped isotope analysis has the potential to be used for estimating the formation temperature of N_2O in industrial processes such as nitric acid synthesis (800 – 900 °C), municipal waste combustion (500 – 1000 °C), or catalytic converters (DeNO$_x$ catalysts, 200 °C).

In addition, clumped isotopes provide unique information about the reversibility of a process,[21] and thus assist in disentangling biogeochemical production pathways, e.g. fungal denitrification[22] and hydroxylamine oxidation,[23] which are largely unresolved with the conventional isotope approaches.

Furthermore, quantum mechanical calculations of ultraviolet absorption cross sections predict fractionation of the clumped N_2O isotopes by its main destruction process, photolysis in the stratosphere.[24,25] In order to trace these processes, e.g. to resolve a difference of 10 °C in formation temperature (at 100 – 200 °C) or to study photolytic N_2O destruction, the instruments need to be capable of detecting changes of δ values of less than 1 ‰ in δ548 and δ458 and 0.1 ‰ in δ556.[18]

The first analysis of the two most abundant clumped isotopic species of N_2O, 458 and 548, has been recently performed by high resolution gas source isotope ratio mass spectrometry (IRMS, type MAT253 Ultra).[16] The reported measurement precision was about 0.10 ‰ for $\delta^{15}N^{bulk}$, $\delta^{17}O$, $\delta^{18}O$, and $\delta^{15}N^a$, and 0.70 to 1.30 ‰ for SP^{18} using 10 µmol of pure N_2O. The mass spectrometric techniques have a fundamental limitation in separating molecules with the same mass, e.g. the two isotopomers 458 and 548. For singly substituted isotopic species, this problem can be resolved by analyzing NO^+ fragment and N_2O^+ molecular ions separately. This, however, is complicated by rearrangement of the nitrogen atoms (N^α and N^β) in the ion source of the mass spectrometer. The rearrangement, or so called isotope scrambling,[8] requires the implementation of complex correction schemes and increases the uncertainty of the method.

Mid-infrared (mid-IR) laser absorption spectroscopy is a direct method for the site-specific analysis of singly and doubly substituted isotopocules of GHGs. The method is inherently selective, even for molecules with the same mass but different position-specific isotopic substitution (isotopomers), and offers high measurement sensitivity by accessing the strong fundamental rovibrational transitions of the molecules. With the advent of quantum cascade lasers (QCLs), a number of applications have been realized, including high precision isotope ratio measurements for singly substituted isotopocules of CO_2,[26] CH_4,[27] and N_2O.[28] Moreover, laser spectroscopy has been recently applied to clumped isotopes in CH_4 (CH_3D, CH_2D_2)[29,30] and CO_2 ($^{13}C^{16}O^{18}O$).[31,32] However, no spectroscopic method has been developed so far for measuring clumped isotopocules of N_2O.

Here we extend the laser analytical technique towards the selective and simultaneous measurement of the eight most abundant isotopocules of N_2O – the main isotopocule 446, all the singly substituted isotopocules 456, 546, 447, and 448, and three clumped isotopocules 458, 548, and 556 – using a high-resolution dual-laser QCL absorption spectrometer (QCLAS). The assignment of spectral lines is confirmed by standard addition of in-house synthesized pure clumped N_2O. For referencing N_2O isotopocule concentrations to the international isotope ratio scales and stochastic distribution, we developed a new scheme by combining thermal equilibration and mole fraction-calibration. The QCLAS technique shows competitive or superior precision to the currently prevailing high-resolution IRMS and, in addition, offers the advantage of inherent selectivity, real-time data coverage, and capability for on-site operation. Finally, being a non-destructive technique, the samples can be fully recovered for re- or further analysis. This is especially important for applications with limited sample size.

METHODS

Selection of spectral regions

To define the wavelength of the lasers to be used in the instrument, the position of spectral lines had to be determined. Supplementary Figure 1 shows the absorption bands of the asymmetric stretching vibration ν_3 for ten N_2O isotopocules in the spectral region between 2100 and 2260 cm^{-1}. Data for 446 and singly substituted isotopocules originate from the HITRAN 2012 database.[7] Line positions and line strengths for doubly substituted isotopocules 556, 458, and 548, as well as 457 and 547, have been simulated using the software PGOPHER[33] as these data were not available in any spectral database at the beginning of this work. PGOPHER predicts the effective Hamiltonian of a molecule from rotational and centrifugal distortion constants. These parameters are available in literature for isotopocules 556,

458, 548, 457, and 547 for the ground-state band 0001–0000 (see Supplementary Table 2).[34–36] To verify the PGOPHER simulations, we simulated the line positions of the isotopocules 446, 456, 546, 448, and 447 with the same procedure and compared them with data published in the HITRAN[7] and GEISA[37] databases. The maximal difference between the simulated lines and line positions in the databases is 0.0012 cm^{-1}. Thereafter, we selected two spectral ranges at 2142 and 2182 cm^{-1} that offer comparable line intensities for all the studied N_2O isotopocules and no spectral interferences from other major atmospheric trace gases, mainly CO, CO_2, H_2O, and CH_4. Due to their spectral interference with the main isotopocule 446, the isotopocules 457 and 547 cannot be analyzed in the spectral ranges selected for this study.

The simulated line positions of the clumped species were validated using high-purity N_2O with natural isotopic composition. The gas was incrementally enriched with either pure 458, 548, or 556 N_2O (synthesized in-house, see below) using a set of mass-flow controllers (red-y MFC; Vögtlin Instruments GmbH, Aesch, Switzerland) to generate a dynamic gas mixture (Supplementary Fig. 2). The concentration of the respective clumped species was increased stepwise to five times their natural isotopic abundance. The spectra were examined for consistency of peak assignment and possible interference effects of allocated and unknown lines of clumped isotopocules on the other analyzed species.

QCLAS spectrometer
A commercial dual-laser QCLAS instrument (Aerodyne Research Inc., Billerica, MA, USA; QCLAS I) was modified for this study with two QCL sources (Alpes Lasers SA, St-Blaise, Switzerland). Laser 1 operating at 2142 cm^{-1} enables simultaneous analyses of isotopocules 446, 456, 546, and 556 (Fig. 1A) and laser 2 emitting at 2182 cm^{-1} is used to analyze 548 and 458, and also 446, 447, and 448 (Fig. 1B). The spectrometer is equipped with a 2.5 L volume astigmatic Herriott multi-pass absorption cell. The recorded absorption spectra were fit with a Gaussian-convoluted Voigt profile, taking into account the optical path length (204 m), the gas temperature (290 K) and pressure (4 hPa) in the absorption cell and the laser line width (approx. 0.001 cm^{-1}) to retrieve fractional amounts of isotopocules, with the baseline treated as a low-order polynomial. Laser scanning, signal processing, and quantitative spectral fitting are realized with the software TDLWintel (Aerodyne Research, Inc., Billerica, MA, USA). The measured fractional amounts of isotopocules are normalized to the abundance of the species 446. A second, single-laser QCLAS analyzer (Aerodyne Research Inc., Billerica, MA, USA; QCLAS II) operating at 2203 cm^{-1} was used for supportive analysis of singly substituted N_2O isotopocules.[23]

Synthesis of 556, 458, and 548
For confirmation of line positions and for thermal equilibration experiments, gas samples of pure doubly substituted N_2O isotopocules 556, 458, and 548 were prepared by thermal decomposition of correspondingly doubly labelled ammonium nitrate salts (NH_4NO_3), according to Eq. 2 to 4:[8]
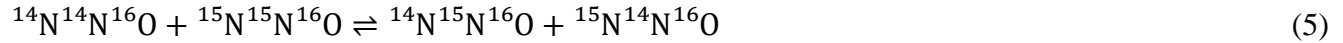
$$^{15}NH_4\,^{15}N^{16}O_3 \rightarrow\, ^{15}N^{15}N^{16}O + 2H_2\,^{16}O \tag{2}$$

$$^{14}NH_4\,^{15}N^{18}O_3 \rightarrow\, ^{14}N^{15}N^{18}O + 2H_2\,^{18}O \tag{3}$$

$$^{15}NH_4\,^{14}N^{18}O_3 \rightarrow\, ^{15}N^{14}N^{18}O + 2H_2\,^{18}O \tag{4}$$

As shown above, the nitrogen atom at the α position of product N_2O originates from the NO_3^- anion, while the β nitrogen comes from the NH_4^+ cation. Ammonium nitrate $^{15}NH_4^{15}N^{16}O_3$ (98 % ^{15}N enrichment) was purchased from Sigma-Aldrich Chemie GmbH (Buchs, Switzerland). Ammonium nitrates labelled with both ^{15}N and ^{18}O were not commercially available and were synthesized in-house by first exchanging the oxygen of nitric acid HNO_3 with ^{18}O-labelled H_2O (80 % ^{18}O, Sigma-Aldrich Chemie GmbH, Buchs, Switzerland) and subsequent reaction with NH_3 to NH_4NO_3 using the procedure described in Supplementary Method 1. Experimental details on the thermal decomposition of NH_4NO_3 to N_2O are given in Supplementary Method 2.

The isotopic purity of the synthesized gases was tested using a quadrupole mass spectrometer (MKS Instruments, Munich, Germany). The gas decomposed from the commercial $^{15}NH_4^{15}N^{16}O_3$ contains mainly the isotopocule 556 (95.5 % mass 46 – species 556; 4.4 % mass 45 – species 456 and 546; 0.1 % mass 44 – species 446). Decomposition of the synthesized $^{14}NH_4^{15}N^{18}O_3$ and $^{15}NH_4^{14}N^{18}O_3$ salts provided the target 458 (53.6 %) and 548 (54.3 %) isotopocules, respectively, as well as the ^{16}O labelled isotopocules, 456 (46.4 %) and 546 (45.7 %), respectively. The anticipated presence of residual 456 and 546 is due to the $^{18}O/^{16}O$ content of the used ^{18}O-labelled water and the exchange equilibrium between HNO_3 and H_2O. As the natural abundance of 456 and 546 is a factor of 500 higher than the abundance of 458 and 548 (cf. Supplementary Table 1), residual 456 and 546 in the 458 and 548 enriched gases, respectively, do not impair the described applications.

The Δ notation for clumped N_2O

Isotope exchange between the twelve N_2O isotopocules, in accordance with Wang et al.,[18] can be described by eight equilibrium reactions. Eq. 5 provides the equilibrium reaction e.g. between the doubly substituted isotopocule 556 and the most abundant 446, with the equilibrium constant K (Eq. 6). A formula for computing Δ556 (Eq. 7), from K and K^* (constant at stochastic composition) can be defined following principles described in the literature; a detailed and illustrative description is provided e.g. by Prokhorov et al. for CO_2[38] and Ono et al. for CH_4.[29] Δ458 and Δ548 are derived in like manner.

$$^{14}N^{14}N^{16}O + {}^{15}N^{15}N^{16}O \rightleftharpoons {}^{14}N^{15}N^{16}O + {}^{15}N^{14}N^{16}O \tag{5}$$

$$K = \frac{[456][546]}{[446][556]} \tag{6}$$

We define

$$\Delta 556 = -\ln\left(\frac{K}{K^*}\right) = \left(\frac{R556}{R556^*} - 1\right) - \left(\frac{R456}{R456^*} - 1\right) - \left(\frac{R546}{R546^*} - 1\right). \tag{7}$$

R556 is the ratio of the abundance of isotopocule 556 relative to 446 in a sample, while R556* is the abundance ratio in the same sample gas but with stochastic (random) distribution of isotopes and serves as a reference point. R556*, R546*, and R456* can be obtained from the total abundance (concentration) of isotopes ^{14}N and ^{15}N as given in Eq. 8 to 10, respectively.

$$R556^* = \frac{[556]^*}{[446]^*} = \frac{[^{15}N]^2[^{16}O]}{[^{14}N]^2[^{16}O]} = \frac{[^{15}N]^2}{[^{14}N]^2} \tag{8}$$

$$R456^* = \frac{[456]^*}{[446]^*} = \frac{[^{15}N]}{[^{14}N]} \tag{9}$$

$$R546^* = \frac{[546]^*}{[446]^*} = \frac{[^{15}N]}{[^{14}N]} \tag{10}$$

In practice, measurements are usually referenced against a working standard gas (*wstd*). In Eq. 11, we exchange $\Delta556$ from Eq. 7 by $\Delta^{556}_{sample/stoch}$, and extend the formula in agreement with Werner et al.:[39]

$$\Delta^{556}_{sample/stoch} = \delta^{556}_{sample/stoch} - \delta^{456}_{sample/stoch} - \delta^{546}_{sample/stoch} = \delta^{556}_{sample/wstd} - \delta^{456}_{sample/wstd} - \delta^{546}_{sample/wstd} + \Delta^{556}_{wstd/stoch} + \delta^{556}_{sample/wstd} \cdot \delta^{556}_{wstd/stoch} \cdot 10^{-3} - \delta^{456}_{sample/wstd} \cdot \delta^{456}_{wstd/stoch} \cdot 10^{-3} - \delta^{546}_{sample/wstd} \cdot \delta^{546}_{wstd/stoch} \cdot 10^{-3} \tag{11}$$

where $\delta_{sample/wstd}$ values are referred to the *wstd* and a correction for a Δ value of the *wstd* is applied ($\Delta^{556}_{wstd/stoch}$, Eq. 12). The multiplicative terms $\delta_{sample/wstd} \cdot \delta_{wstd/stoch} \cdot 10^{-3}$ can be ignored for simplicity, which causes a difference of below 0.5 ‰ for samples with natural isotopic abundances but above 1 ‰ for enriched samples. To obtain the $\Delta_{wstd/stoch}$ values, the *wstd* has to be analyzed versus the thermally equilibrated working standard ($\delta_{wstd/eq}$) and then related to its stochastic composition ($\delta_{eq/stoch}$) using theoretical predictions[18] following the additive theorem for δ-notation (used also in derivation of Eq. 11), e.g. for $\Delta^{556}_{wstd/stoch}$:

$$\Delta^{556}_{wstd/stoch} = \delta^{556}_{wstd/stoch} - \delta^{456}_{wstd/stoch} - \delta^{546}_{wstd/stoch} = \delta^{556}_{wstd/eq} + \delta^{556}_{eq/stoch} + \delta^{556}_{wstd/eq} \cdot \delta^{556}_{eq/stoch} \cdot 10^{-3} - (\delta^{456}_{wstd/eq} + \delta^{456}_{eq/stoch} + \delta^{456}_{wstd/eq} \cdot \delta^{456}_{eq/stoch} \cdot 10^{-3}) - (\delta^{546}_{wstd/eq} + \delta^{546}_{eq/stoch} + \delta^{546}_{wstd/eq} \cdot \delta^{546}_{eq/stoch} \cdot 10^{-3}) \tag{12}$$

Thermal equilibration

For the thermal equilibration, a natural abundance N_2O (99.999 %, Messer Schweiz AG, Switzerland) was spiked with one of the three in-house synthesized doubly substituted N_2O isotopocules (556, 458, or 548) to 50 % above their natural abundance, in order to trace the progress of equilibration in time. 250 µmol of the spiked N_2O gas was flame-sealed into a quartz-glass tube (outer diameter 9 mm, length 220 mm) that was filled with 400 mg of aluminium oxide (activated, neutral, type Brockmann I; Sigma-Aldrich Chemie GmbH, Buchs, Switzerland) and topped with silanized glass wool (Sigma-Aldrich Chemie GmbH, Buchs, Switzerland). Before introducing N_2O, the catalyst was heated in the tube attached to a vacuum line with propane flame until the pressure in the system dropped below 0.3 hPa. After filling with N_2O and flame-sealing, the tubes were placed into a muffle furnace for a specified time. The equilibration experiments were done at 100 °C (55 – 790 hours), 200 °C (2.5 – 116 hours), 300 °C (16 hours), 400 °C (20 hours), and 500 °C (46 – 240 hours) with all three spiked N_2O gases. Equilibration at 100 °C was initiated by heating at 200 °C for 14 – 16 hours before the temperature was decreased to 100 °C.[16] After the respective time period at the equilibration temperature, the tubes were taken out of the furnace and quenched immediately in a cold pressurized air flow. The gases were then purified on the vacuum line where N_2O was condensed at 77 K (liquid N_2), while N_2 and O_2 were removed by evacuation with an oil sealed rotary vane pump. The purified equilibrated N_2O gases were analyzed by QCLAS I in triplicate versus the unequilibrated gas mixtures to investigate the progress of equilibration. A single-point offset correction scheme on δ values was applied, as no second calibration gas with known isotopic composition for clumped isotopocules was available at that point in time.

The data was fitted using exponential functions – for δ^{456} and SP, the saturation function $y = a \cdot (1 - e^{-x/b})$ was used, where y is δ^{456} or SP value, a is a saturation value at long times (in ‰), x is the equilibration time (t_{eq} in Fig. 2), and b is a time constant of the saturation (in hours). For δ^{546} and δ(spike), the decay function $y = a \cdot (e^{(-x/b)}) + c$ was applied, where y is δ^{546} or δ(spike) value, a and c are intercepts (in ‰), x is the equilibration time, and b is a time constant of the decay (in hours).

Combined mole fraction-calibration scheme

The new reference frame for N_2O isotopocules was established by combining thermal equilibration and mole fraction-calibration. In a first step, mole fractions of the clumped species in the *wstd* gas (high purity N_2O, 99.999 %, PanGas – The Linde Group, Dagmersellen, Switzerland) were obtained. In order to do so, $\delta^{458}_{wstd/eq}$, $\delta^{548}_{wstd/eq}$, and $\delta^{556}_{wstd/eq}$ values were retrieved by analysis of the *wstd* against the equilibrated *wstd* gas. δ values for the singly substituted N_2O isotopocules of the working standard were determined by QCLAS II against reference gases, previously anchored to the international isotope ratio scales by Sakae Toyoda at Tokyo Institute of Technology (Yokohama, Japan).[8] These values were used as input variables for theoretical predictions of $\delta_{eq/stoch}$.[18] Detailed description is provided in section Results (Clumped isotope calibration strategies, part B).

In a second step, a set of seven high-accuracy gravimetric mixtures of the N_2O working standard in N_2 (purity 99.9999 %) was prepared by the National Physical Laboratory (NPL, Teddington, UK). The concentration of the calibration gases (CGs) ranges from 1.50 to 1.85 % N_2O in N_2 (CG1 – CG7; Supplementary Table 3) to bracket the expected enrichment or depletion of individual isotopocules in natural samples (Supplementary Table 4). Production of the CGs at NPL included the preparation of an intermediate gravimetric mixture of 12 % N_2O in N_2 that was consecutively diluted to the target N_2O mole fractions of CG1 – CG7 (Supplementary Table 3). The N_2O mole fractions of the CGs were validated by an additional gravimetric dilution to 325 nmol mol^{-1} in synthetic air and subsequent analysis against NPL in-house standards by cavity ring-down spectroscopy (G5131 I; Picarro Inc., Santa Clara, CA, USA). Possible fractionation effects during production of the CGs were excluded by analysis of CG1 – CG7 by QCLAS II against reference gases anchored to the international scales.[8] Prior to analysis, all gases were diluted to 100 µmol mol^{-1} N_2O in synthetic air (20.5 % O_2 in N_2; Messer Schweiz AG, Lenzburg, Switzerland). The isotopic standards used by QCLAS II for the analysis of the CGs and their original pure N_2O gas were: (1) $\delta^{15}N^\alpha = (2.06 \pm 0.05)$ ‰; $\delta^{15}N^\beta = (1.98 \pm 0.20)$ ‰; $\delta^{18}O = (36.12 \pm 0.32)$ ‰; and (2) $\delta^{15}N^\alpha = (-48.59 \pm 0.25)$ ‰; $\delta15N^\beta = (-46.11 \pm 0.43)$ ‰; $\delta^{18}O = (27.37 \pm 0.11)$ ‰. The standards used for the analysis of the VG1 and its original pure N2O gas were: (1) $\delta^{15}N^\alpha = (25.73 \pm 0.24)$ ‰; $\delta^{15}N^\beta = (25.44 \pm 0.36)$ ‰; $\delta^{18}O = (35.86 \pm 0.22)$ ‰; and (2) $\delta^{15}N^\alpha = (-48.59 \pm 0.25)$ ‰; $\delta^{15}N^\beta = (-46.11 \pm 0.43)$ ‰; $\delta^{18}O = (27.37 \pm 0.11)$ ‰. The uncertainty is expressed as expanded standard uncertainty at the 95 % confidence interval.

Analytical results by QCLAS II for the pure working standard agree with δ values of CG1 – 7 (cf. Supplementary Table 3) within their expanded uncertainty limits, which demonstrates that no significant isotopic fractionation was introduced during the gas mixture preparation by NPL. For the clumped isotopocules, similar behavior, i.e. the absence of fractionation effects during preparation of CG1 – CG7, is assumed. Therefore, δ values of the pure working standard were applied for all gas mixtures in the mole fraction-calibration scheme.

Validation of the N_2O reference frame
In order to validate the new reference frame, two validation strategies were applied: (1) a gravimetric gas mixture with 1.53 % N_2O (gas VG1) with different isotopic composition was produced by NPL using a similar strategy as described above for the calibration gases; (2) three validation gases (VG2,

VG3, VG4) were thermally equilibrated in triplicate at 100 and 200 °C and purified according to the previously described procedure. The preparation of VG2, VG3, VG4 from pure, commercially available N_2O by volumetric doping with defined amounts of isotopically pure (> 98 %) $^{14}N^{15}N^{16}O$ (NLM 1045 PK), $^{15}N^{14}N^{16}O$ (NLM 1044 PK) (Cambridge Isotope Laboratories, Tewksbury, MA, USA) and $^{14}N^{14}N^{18}O$ (in-house synthesized) using a ten port two position valve (EH2C10WEPH with 20 mL sample loop, Valco Instruments Inc., Schenkon, Switzerland) and synthesis of $^{14}N^{14}N^{18}O$ are described elsewhere.[40]

The measurement sequence applied during the validation experiments was initiated by analysis of CG1, CG5, and CG7 followed by triplicate analysis of a sample and final repeated analysis of CG1, CG5, and CG7. Average values for the CGs were used for the calibration, which reduces also potential drift between the analysis of CGs and the sample. The full sequence was repeated five times for VG1 and once for all three subsamples of VG2 – VG4 equilibrated individually.

High-resolution mass-spectrometric measurements
The isotopic composition of the equilibrated samples VG2, VG3, and VG4 was also determined by high resolution isotope ratio mass spectrometry with a MAT253 Ultra (Thermo Scientific, Bremen, Germany, here labelled as HR-IRMS) at Tokyo Institute of Technology (Yokohama, Japan). The measurement was made using previously published methods for site specific ^{15}N analysis and clumped isotope analysis.[16] The method consists of three separate analyses of NO^+ fragment ions and N_2O^+ molecular ions of the singly and doubly substituted isotopocules, all performed at mass resolutions of approx. 16,000 – 19,000 using a 16 µm slit (middle resolution). For each set of measurements, the detectors were positioned such that the flat tops of every peak of interest were aligned. All measurements were made in dual-inlet mode. Every sample and standard intensity comparison ('acquisition') was composed of 8 cycles with 8 s integration time for each individual measurement. The measurement was performed with 9.9 kV accelerating voltage, filament emission current of 1.65 mA, and equilibration time of 35 s. Before each acquisition, a series of 500 s background scans was collected for both sample and reference gases. More information is available in Supplementary Method 3. The Δ values provided by HR-IRMS were referenced to a working standard used at Tokyo Institute of Technology ($\delta^{15}N^{\alpha} = (-4.07 \pm 0.06)$ ‰, $\delta^{15}N^{\beta} = (-0.02 \pm 0.14)$ ‰, $\delta^{18}O = (20.63 \pm 0.12)$ ‰). The uncertainty is expressed as expanded standard uncertainty at the 95 % confidence interval. As the $\Delta_{wstd/stoch}$ was not known, no correction to stochastic distribution for the doubly substituted species 458 and 548 could be applied. Instead, a correction based on Eq. 29 was applied.

RESULTS

Spectral regions and analysis
The spectral ranges for the eight most abundant N_2O isotopocules were identified using PGOPHER simulations[33] in combination with spectral data from the database HITRAN.[7] Two distinct spectral windows at 2142 and 2182 cm^{-1} (Fig. 1A for laser 1 and Fig. 1B for laser 2, respectively) were selected, offering comparable line intensities for all the studied N_2O isotopocules and having no spectral interferences from other major atmospheric trace gases. Spectral simulations indicate that the absorption of the interferents is below 1 ‰ of N_2O absorption (for 1 % N_2O) up to 30 ppm CO, 2000 ppm CO_2, 6 % H_2O, 5 % CH_4, and 15 ppm O_3. The line parameters for the spectroscopic measurements using the dual-laser QCLAS (further denoted as QCLAS I) are given in Supplementary Table 5.

The line positions simulated for the clumped species were validated with a number of standard addition experiments. For this, N_2O of natural isotopic composition was supplemented with either synthesized pure 458, 548, or 556 species (Supplementary Fig. 2). Based on these experiments, the

calculated absorption lines of clumped species were confirmed in both spectral regions. In addition, one previously unknown line of the 458 isotopocule was identified at 2142.647 cm^{-1}.

Optimized experimental conditions and achieved precision
The sensitivity of the QCLAS can be enhanced by increasing the absorption signal, i.e. improving the signal-to-noise ratio either by using higher pressure or increasing the amount fraction of the absorbing molecules. For isotope ratio analysis, however, it is equally important to achieve excellent selectivity and minimize spectral interferences. Generally, low cell pressure is beneficial as it reduces the pressure broadening of absorption lines and thereby interferences between adjacent spectral lines or molecular transitions. This is of particular importance for laser 2, where a strong neighboring line of 446 at 2182.670 cm^{-1} (outside of the plotted range in Fig. 1B) with a spectral line intensity of $1.064 \cdot 10^{-19}$ cm^{-1}/(molecule cm^{-2}) affects the baseline with increasing pressure. Therefore, experimental conditions for QCLAS I, especially the minimal required amount of N_2O and pressure in the optical cell, were optimized. Figure 3A indicates that the best Allan precision[41] for δ548 with 1 s spectral averaging can be achieved with 3 – 4 µmol of N_2O irrespective of the applied cell pressure (between 1 and 7 hPa) and matrix gas (He, N_2). Similarly, the best precision for δ458 and δ556 was reached with 5 and 7 µmol of N_2O, respectively.

Thus, the optimal measurement conditions were selected: cell pressure of 4 hPa using approx. 4 µmol of N_2O in a N_2 gas matrix. Under these conditions, a precision of < 0.40 ‰ for δ548, $0.20 – 0.30$ ‰ for δ556, $0.10 – 0.20$ ‰ for δ458, δ448, δ447, and 0.10 ‰ for δ456 and δ546 (Fig. 3B and 3C) was achieved for integration times of 600 – 1000 s for laser 1 and of 30 – 100 s for laser 2, respectively. The precision was derived from the square root of the Allan variance.

Clumped isotope calibration strategies
An often underestimated challenge of clumped isotope ratio measurements is the construction of a primary reference scale, which has not been set up so far for clumped N_2O isotope analysis. We implemented two alternative, independent approaches: (A) to equilibrate a gas mixture at selected temperatures to adjust clumped isotopocule abundances,[18] (B) to calibrate individual isotopocule mole fractions using high accuracy gravimetric mixtures,[42,43] which are described in detail below. The first approach follows principles of statistical thermodynamics in order to evaluate the equilibrium constants of isotope exchange reactions (e.g. Eq. 5) and to calculate the proportions of all isotopocules that are consistent with the bulk isotopic composition.[18] Abundances of clumped isotopocules deviate from the stochastic distribution as a function of temperature (1/T), which is the basis of their use as geothermometers. In return, this is the standard technique for calibration in clumped isotope science.

However, for N_2O the equilibration approach has some limitations, e.g. only small sample volumes can be equilibrated, and equilibration succeeds only in a limited temperature range. At the low temperature side, extensive hold times are required, while at higher temperatures thermal decomposition occurs. The second calibration approach, developed for optical analyzers, overcomes these limitations as high-pressure cylinders with calibration gases can be prepared, and a single N_2O isotopic quality diluted to different mole fractions enables multi-point calibration. However, as a requirement, N_2O gas with defined abundances of clumped isotopocules is required. In the presented study, we combine the advantages of both approaches: we use the thermal equilibration to provide a reference point for the abundance of clumped isotopocules, and we propagate this information to N_2O gas applied in the mole-fraction based calibration scheme.

A) Thermal equilibration of N_2O

Firstly, N_2O was thermally equilibrated using high-surface-area alumina (Al_2O_3) following Magyar et al.[16] and the results were compared to the theoretical predictions of Wang et al.[18] Three mixtures of high-purity N_2O, each mixture spiked with only one of the in-house synthesized pure clumped species (458, 548, or 556) to 50 % above natural abundance, were used to validate the equilibration procedure and to optimize experimental conditions.

Complete thermal equilibration of N_2O was confirmed for the first two spiked gas mixtures after 48 hours at 200 °C and after 180 hours at 100 °C by the disappearance of the respective clumped isotopocule enrichment (Fig. 2A and 2B), while the 556 spike remained unchanged (Fig. 2C). Additionally, thermodynamic equilibrium of the N–O bond is indicated by the emergence of a stable difference in the ^{15}N substitution between α and β position, i.e. stable SP and SP[18]. Figure 2D shows the change of SP during the equilibration experiments and confirms equilibration of the N–O bond in all three spiked gas mixtures. Exponential fitting of the data result in average time constants (*e*-folding times) for δ456 of (20.55 ± 9.68) h at 100 °C and (3.49 ± 0.58) h at 200 °C, and for δ546 of (25.25 ± 14.09) h at 100 °C and (2.80 ± 0.90) h at 200 °C, respectively.

The ^{15}N substituted isotopocules in the equilibrated gases were additionally analyzed using a single-laser QCLAS system (further denoted as QCLAS II) with reference to the Air-N_2 scale provided by the Tokyo Institute of Technology[8] (Table 1). A good agreement in SP was found between the two spectroscopic techniques but, in particular for gases equilibrated at 100 °C, experimental results show 4 – 5 ‰ deviation from theoretical predictions.

B) Calibration based on individual isotopocule mole fractions

A second calibration strategy, recently suggested for singly substituted isotopocule analysis by infrared optical analyzers,[42,43] was modified for the clumped N_2O isotopes. This approach, which relies on high-accuracy gravimetric calibration gases, is based on the calibration of individual isotopocule mole fractions rather than conventional calibration of isotopocule ratios or δ values. The δ values of the calibration gases (CGs; NPL, Teddington, UK) for singly substituted isotopic species were assigned against international isotope ratio scales by QCLAS II. $\delta_{wstd/stoch}$ values of doubly substituted isotopic species were derived from the analysis of the *wstd* against the same gas that was thermally equilibrated at 200 °C and relating it to stochastic distribution following Eq. 12. This step signifies the essential connection between the two calibration strategies. Based on the Eq. 12 and the thermal equilibration experiments, $\Delta_{wstd/stoch}$ values were determined as: $\Delta^{458}_{wstd/stoch} = (-0.06 \pm 0.80)$ ‰, $\Delta^{548}_{wstd/stoch} = (0.49 \pm 0.46)$ ‰, $\Delta^{556}_{wstd/stoch} = (-0.88 \pm 1.76)$ ‰ (expanded uncertainties at the 95 % confidence interval, propagated from standard error of the mean for repeated measurement of all δ values in Eq. 12, N=9).

In order to set up the mole fraction-calibration scheme, ratios of individual singly substituted isotopocules R456, R546, R447, and R448 were calculated from δ values of the CGs, e.g.:

$$R456 = R^{15}_{N2-AIR}(1 + \delta^{15}N^\alpha) \tag{13}$$

$$R447 = R^{17}_{VSMOW}(1 + \delta^{18}O)^\lambda \tag{14}$$

where R^{15}_{Air-N2}, R^{17}_{VSMOW}, and R^{18}_{VSMOW} are $^{15}N/^{14}N$, $^{17}O/^{16}O$, and $^{18}O/^{16}O$ ratios of tropospheric N_2 (Air-N_2) and VSMOW, respectively, and λ is the mass-dependent factor that relates differences in ^{17}O and ^{18}O abundances.[39] Ratios of doubly substituted isotopocules R458, R548, and R556 were derived from δ values of the *wstd* normalized against stochastic distribution (obtained by thermal equilibration experiments based on Eq. 12), e.g.:

$$R548 = R_{stoch}^{548}\left(1 + \delta_{wstd/stoch}^{548}\right) \tag{15}$$

where $R^{548}{}_{stoch}$ is the ratio of 548 over 446 in the working standard with stochastic distribution of isotopes. Then, atomic isotopic abundances were calculated following Eq. 16 – 22:

$$X\left(^{14}N, \alpha\right) = \frac{1}{1+R456} \tag{16}$$

$$X\left(^{15}N, \alpha\right) = \frac{R456}{1+R456} \tag{17}$$

$$X\left(^{14}N, \beta\right) = \frac{1}{1+R546} \tag{18}$$

$$X\left(^{15}N, \beta\right) = \frac{R546}{1+R546} \tag{19}$$

$$X\left(^{16}O\right) = \frac{1}{1+R447+R448} \tag{20}$$

$$X\left(^{17}O\right) = \frac{R447}{1+R447+R448} \tag{21}$$

$$X\left(^{18}O\right) = \frac{R448}{1+R447+R448} \tag{22}$$

Using the atomic isotopic abundances and the N_2O mole fractions (x_{N2O}), mole fractions of isotopocules in the CGs x_{446}, x_{456}, x_{546}, x_{447}, and x_{448} were derived, e.g.:

$$x_{446} = \left[X(^{14}N, \alpha) \cdot X(^{14}N, \beta) \cdot X(^{16}O)\right] \cdot x_{N_2O} \tag{23}$$

$$x_{456} = \left[X(^{14}N, \alpha) \cdot X(^{15}N, \beta) \cdot X(^{16}O)\right] \cdot x_{N_2O} \tag{24}$$

For the clumped isotopocules, the ratios $R458$, $R548$, and $R556$ obtained following Eq. 15 were converted to mole fractions x_{458}, x_{548}, and x_{556}, e.g.:

$$x_{548} = R548 \cdot x_{446} \tag{25}$$

Calculated (x_{xyz}) and analyzed (y_{xyz}) mole fractions of isotopocules in the CGs were used to derive in total 9 linear calibration functions (laser 1 – species 446, 456, 546, 556; laser 2 – species 447, 448, 446, 548, 458) in accordance with Flores et al.[43] Slope a and intercept b of the linear calibration functions were retrieved by linear regression and used to calculate isotopocule mole fractions in a sample gas ($x_{xyz,sam}$) from the corresponding calibration equation:

$$x_{xyz,sam} = \frac{y_{xyz,sam}-b}{a} \tag{26}$$

where $y_{xyz,sam}$ is the mole fraction of an isotopocule xyz in a sample measured by QCLAS I (Supplementary Fig. 3). Finally, the mole fractions $x_{xyz;sam}$ were used to calculate δ values in a sample related to the international isotope ratio scales or stochastic distribution, e.g.:

$$\delta456 = \frac{\frac{x_{456,sam}}{x_{446,sam}}}{R^{15}_{N_2-AIR}} - 1 \tag{27}$$

$$\delta548 = \frac{\frac{x_{548,sam}}{x_{446,sam}}}{R^{15}_{N_2-AIR} \cdot R^{18}_{VSMOW}} - 1 \tag{28}$$

Validation and uncertainty assessment of the combined mole fraction-calibration scheme

Detailed validation and uncertainty assessment were conducted for the combined mole fraction-calibration scheme described above. At first, δ values for singly substituted isotopocules analyzed by QCLAS I for a high-accuracy gravimetric validation gas VG1 were compared to values provided by an established analytical approach using QCLAS II with the conventional δ-calibration (Table 2, upper part – VG1). The differences between the values assigned by QCLAS I and II, calculated as $\Delta_{I-II} = \delta_{QCLASI} - \delta_{QCLASII}$, were: $\Delta^{456}_{I-II} = (-0.29 \pm 0.55)$ ‰, $\Delta^{546}_{I-II} = (-0.53 \pm 0.64)$ ‰, $\Delta^{448}_{I-II} = (1.21 \pm 0.64)$ ‰. The larger difference in Δ^{448}_{I-II} is caused by an underestimation of $\delta^{18}O$ by QCLAS II, as $\delta^{18}O$ of VG1 lies outside the $\delta^{18}O$ range of available standard gases for QCLAS II. This was already observed earlier[44] and is confirmed by $\delta^{18}O$ analysis of VG1 by IRMS at Max Planck Institute for Biogeochemistry (Jena, Germany; Table 2, $\Delta^{448}_{I-IRMS} = (-0.83 \pm 0.51)$ ‰). The uncertainty is expressed as the expanded standard uncertainty at the 95 % confidence interval.

In a second validation approach, N_2O gases with no (VG2), strong (50 ‰, VG3) and very strong (100 ‰, VG4) enrichment in the singly substituted isotopocules 456, 546, and 448 were thermally equilibrated at 100 and 200 °C. As a part of the validation, the gases were measured by the presented QCLAS I and also by the competitor high-resolution IRMS instrument (MAT253 Ultra, Tokyo Institute of Technology, Tokyo, Japan; denoted as HR-IRMS onwards). Thereby, the linearity of both instruments over a wide range of $\delta^{15}N^{bulk}$ and $\delta^{18}O$ values was intercompared. Moreover, results for equilibrated VG2, VG3, and VG4 at 200 °C by QCLAS I and HR-IRMS analyses were compared to theoretical predictions (Table 2 and Fig. 4). The theoretical predictions were computed based on equilibrium thermodynamics[18] and the known bulk isotopic compositions of the gases (listed in Methods). As the reference gas used by HR-IRMS was not isotopically characterized for the content of the doubly substituted species, the measured values δ^{458} and $\delta^{458+548}$ at 200 °C for HR-IRMS were referenced to the ratio between the measured and the theoretical δ values at 100 °C:

$$\delta^{458} = \left(\frac{\left(\frac{\delta^{458}_{measured,200\,°C} + 1}{1000} \right)}{\left(\frac{\delta^{458}_{measured,100\,°C} + 1}{1000} \right)} \left(\frac{\delta^{458}_{theory,100\,°C}}{1000} + 1 \right) - 1 \right) \cdot 1000. \tag{29}$$

$\Delta^{458+548}_{avg}$ and SP^{18} presented in Table 2 and Fig. 4 for HR-IRMS were calculated from δ^{458} and $\delta^{458+548}$ values corrected as described in Eq. 29.

Results indicate that the QCLAS I and HR-IRMS reach a similar precision for $\delta^{15}N^{bulk}$ and $\delta^{458+548}_{avg}$, in the range of 0.31 – 0.45 ‰ and 0.49 – 0.56 ‰ (QCLAS I), and 0.14 – 0.15 ‰ and 0.46 – 0.97 ‰ (HR-IRMS), respectively. The precision was expressed as standard deviation for repeated analyses within one measurement run. The average accuracy of QCLAS I and HR-IRMS results of $\delta^{15}N^{bulk}$ and $\delta^{458+548}_{avg}$ values, with respect to theoretical predictions, is 0.28 and 3.84 ‰ (QCLAS I), and 1.50 and

1.92 ‰ (HR-IRMS), respectively. The accuracy was calculated as average difference between the measured and the theoretical value.

The repeatability of QCLAS I results for $\delta^{15}N^{bulk}$ and $\delta^{458+548}_{avg}$ values is 0.14 – 0.20 ‰ and 0.22 – 0.25 ‰, respectively. For HR-IRMS results, it is 0.06 ‰ and 0.19 – 0.40 ‰ for $\delta^{15}N^{bulk}$ and $\delta^{458+548}_{avg}$ values, respectively. The repeatability was calculated as standard deviation of the mean from multiple measurement sequences (see Table 2 for details). There is a clear trend in the $\Delta^{458+548}_{avg}$ with increasing ^{15}N and ^{18}O enrichment (Table 2) for both QCLAS I and HR-IRMS (without the additional referencing by Eq. 29), which could be due to a scale expansion. For laser spectroscopy, this can be caused by the presence of weak absorption lines of either 456, 546, or 448 beneath the 458 and 548 lines, or by incomplete thermal equilibration of oxygen atoms between different N_2O molecules that gets hindered by some so far unknown mechanism.

Regarding site-selectivity, i.e. the difference in abundances between isotopomers 456 versus 546 and 458 versus 548, expressed as SP and SP^{18} (Fig. 4B and 4D, respectively, and Table 2), the average accuracy (deviation from the theoretical value) is 1.62 and 4.26 ‰ for QCLAS I but as high as 3.95 and 10.39 ‰ for HR-IRMS, respectively. This indicates that the measurement of SP^{18} remains a challenge for the IRMS technique, as the HR-IRMS instrument used in this study could not accurately distinguish the two isotopomers 458 and 548 from each other. The repeatability of SP and SP^{18} provided by QCLAS I is in the ranges 0.28 – 0.40 ‰ and 0.44 – 0.50 ‰, respectively. For values obtained by HR-IRMS, it is 0.11 ‰ and 0.37 – 0.79 ‰, respectively. The above results do not include equilibration at 100 °C because of the lower consistency in those results compared to 200 °C, which may be due to incomplete isotope-exchange equilibrium.

In accordance with Flores et al.,[43] the uncertainty of the isotope ratio (R) for a sample gas derived using the combined mole fraction-calibration scheme was estimated from a model equation (Eq. 25; Supplementary Table 6). Taking $R548$ as an example, the uncertainty of the isotopocule (548, 446) mole fractions (x) of a sample gas is derived from the analytical uncertainty of the analyzed mole fractions (y_{548}, y_{446}) and the uncertainty in the slope a and the intercept b of the calibration function. The uncertainty contributions of the latter are derived from the reference values of the CGs (x_{548}, x_{446}) calculated from the uncertainty in N_2O mole fraction, $\delta^{15}N^b$, and $\delta^{18}O$ (Supplementary Table 3) and its analytical uncertainty, estimated from the Allan deviation, using the MATLAB function *linfitxy*.[45] Propagation of uncertainties into the ratio $R548$ results in a relative combined standard uncertainty around 5 ‰. Main uncertainty contributions are allocated to the uncertainties of the slope a and the intercept b of the calibration functions and to a much lower extent to the Allan precision of sample or calibration gas measurements.

DISCUSSION

The QCLAS technique for simultaneous and site selective analysis of the eight most abundant singly and doubly substituted N_2O isotopocules provides a precision of 0.10 – 0.40 ‰ for all δ values using 4 μmol N_2O in a N_2 gas matrix. This is superior to values previously reported using HR-IRMS, achieving 0.10 – 1.30 ‰ with a minimum of 10 μmol N_2O.[16] Another advantage of QCLAS lies in its ability of continuous data collection (typically 1 Hz) over extended periods as compared to discrete sampling and measurement by IRMS. Laser spectroscopic analysis is non-destructive, therefore offers a possibility for recovering the analyte.[30] Furthermore, triplicate analysis of a sample by laser spectroscopy requires 2 hours (the bracketing calibration scheme included), which is much faster than HR-IRMS where the sample is measured in six acquisition blocks for 8 – 10 hours.[16]

Analytical results were related to the stochastic distribution by thermal equilibration of N_2O over high-surface alumina. A progressive decrease in the 458 and 548 but not in the 556 enrichment (Fig. 2)

confirms an isotope-exchange equilibrium for the N–O bond only, in accordance with previous literature.[46,47] It is proposed that the N_2O molecule undergoes reversible adsorption to the surface of Al_2O_3 by the O atom. This results in the weakening and cleavage of the N–O bond and subsequent reversal of the N–N unit. The observed equilibration in the NO moiety only can be rationalized by dissociation energies of the respective bonds. The Gibbs free energy (ΔG) associated with the dissociation of the N–N bond is a factor of four higher than of the N–O bond, e.g. at 200 °C: ΔG_{N-O} = 100.2 kJ mol^{-1}, ΔG_{N-N} = 408.3 kJ mol^{-1}, and persists independently of the presence of a catalyst.

The SP and SP^{18} values of the thermally equilibrated gases with artificial spikes of 458, 548, and 556 (Table 1) gradually approached a constant value in accordance with the work of Magyar et al.[16] A comparison of SP values for equilibration results at 200 °C measured by the two laser spectrometers (QCLAS I, QCLAS II) with reference to the Air-N_2 scale[8] displays a reasonably good agreement with theoretical equilibrium distribution of N_2O isotopocules[18] with differences of up to 2 ‰, within expanded uncertainty limits. For equilibration at 100 °C, analytical results are consistently up to 5 ‰ too low, which may attribute to incomplete equilibration (imprint of preheating) or to inconsistencies of the current reference scale for the N_2O SP.[48] Further equilibration experiments were performed at temperatures up to 500 °C in order to identify alternative equilibration temperatures. However, at temperatures higher than 200 °C, more than 10 % of N_2O is thermally decomposed into N_2 and O_2, which affects the N_2O isotopic composition due to isotopic fractionation. At lower temperatures, i.e. at 100 and 200 °C, more than 95 % of N_2O is retrieved after the equilibration step, minimizing the effect of fractionation on the abundance of isotopocules. Therefore, we suggest that for future referencing of clumped isotopes in N_2O, thermal equilibration experiments should be preferentially performed at 200 °C.

A new calibration scheme was implemented combining thermal equilibration and calibration of individual isotopocule mole fractions using high-accuracy gravimetric mixtures. This represents the first application of a mole fraction-based calibration scheme for clumped isotopes. It has a number of advantages over previous thermal equilibration-based δ-calibration approaches. Namely, only one N_2O source gas is required for multi-point calibration and high volumes of calibration standards can be produced, enabling the frequent calibration that is required for optical analyzers (calibration included in every sample measurement sequence). In addition, no post-correction of the analyzer response for dependencies on N_2O mole fractions is needed, which is a usual requirement using the δ calibration approach in laser spectroscopy.

Parallel measurements of the equilibrated validation gases VG2, VG3, and VG4 by QCLAS I and HR-IRMS indicate similar performance for bulk isotopic composition ($\delta^{15}N^{bulk}$, $\delta^{458+548}_{avg}$), and highlight the advantages of QCLAS for site specificity (SP and SP^{18}). The HR-IRMS results of SP^{18} were largely out of the ranges as predicted by theory, which can be attributed to the current inability of the IRMS technique in differentiating the clumped isotopomers 458 and 548 (Fig. 4D). Such deficiency may be caused by underestimated isotope scrambling in the ion source[8,49] and calls for even more complex correction schemes than those used to date (applied on the values $\Delta^{458+548}_{avg}$ and SP^{18} at 200 °C). Therefore, we recommend to limit the usage of HR-IRMS for SP^{18} only for samples with natural isotopic abundance. On the contrary, the QCLAS technique does not need such corrections because it directly detects both pairs of isotopomers (456–546, 458–548). This is demonstrated by the good agreement between the measured and theoretical SP and SP^{18} values (Fig. 4B and 4D).

The discrepancy of $\Delta^{458+548}_{avg}$ measured with QCLAS I and HR-IRMS with the theoretical predictions of the samples highly enriched in ^{15}N and ^{18}O indicates that oxygen atoms may not be equilibrated in these gases as predicated by statistical thermodynamics. However, the measurements of SP and SP^{18} were consistent with the theoretical results. It is possible that the exchange of oxygen atoms between different N_2O molecules, which determines $\Delta^{458+548}_{avg}$, may not be complete due to an unknown

mechanism. This would call for an alternative equilibration approach for calibration of the $\Delta^{458+548}_{avg}$ value.

Nonetheless, the standard uncertainty of the QCLAS technique for repeated measurements, i.e. 0.1 to 0.2 ‰ for both $\Delta458$ and $\Delta548$, is sufficient to resolve 10 °C temperature differences of thermal production of N_2O, to follow partial destruction by UV photolysis and to study kinetically controlled microbial processes. For $\Delta556$, the current repeatability around 0.6 ‰ is adequate to detect photolytic N_2O destruction and probably microbial disequilibrium processes but has to be further improved to resolve temperature differences in thermal equilibrium processes.

In the spectral regions used by our QCLAS technique, minimal interferences from other atmospheric trace (e.g. CO, CO_2, H_2O, CH_4 or O_3) were identified by spectral simulations. Nonetheless, analysis of environmental samples requires pre-concentration to enhance the N_2O mole fraction,[50] to adjust the gas matrix (N_2), and to remove surplus of other trace gases. Alternatively, correction algorithms can be developed to account for spectral interferences as published by Harris et al.[40]

First applications of the developed QCLAS technique are currently on-going to identify the clumped isotopic signatures of N_2O generated from bacterial nitrification (*Nitrosococcus oceani*) and denitrification (*Pseudomonas aureofaciens*). Furthermore, the imprint of UV photolysis on the clumped isotopic composition will also be assessed. This will provide insight into N_2O sink processes occurring in the stratosphere and an independent proof for theoretical predictions.[24]

REFERENCES

1. P. Forster, Ramaswamy V, Artaxo P, et al. Changes in Atmospheric Constituents and in Radiative Forcing. Chapter 2. In: Solomon S, Qin D, Manning M, et al., eds. *Climate Change 2007: The Physical Science Basis. Contribution of Working Group I to the Fourth Assessment Report of the Intergovernmental Panel on Climate Change*. Cambridge University Press, Cambridge, United Kingdom and New York, NY, USA; 2007. doi:10.1038/nrc3183
2. Ravishankara AR, Daniel JS, Portmann RW. Nitrous oxide (N_2O): the dominant ozone-depleting substance emitted in the 21st century. *Science*. 2009;326(5949):123-125. doi:10.1126/science.1176985
3. World Meteorological Organization, Watch GA. WMO Greenhouse Gas Bulletin (GHG Bulletin) - No. 15. 2019;2018.
4. Thompson RL, Lassaletta L, Patra PK, et al. Acceleration of global N_2O emissions seen from two decades of atmospheric inversion. *Nat Clim Chang*. 2019:1-6. doi:10.1038/s41558-019-0613-7
5. Ostrom NE, Ostrom PH. Mining the isotopic complexity of nitrous oxide: a review of challenges and opportunities. *Biogeochemistry*. 2017;132(3):359-372. doi:10.1007/s10533-017-0301-5
6. Coplen TB. Guidelines and recommended terms for expression of stable-isotope-ratio and gas-ratio measurement results. *Rapid Commun Mass Spectrom*. 2011;25(17):2538-2560. doi:10.1002/rcm.5129
7. Rothman LS, Gordon IE, Babikov Y, et al. The HITRAN2012 molecular spectroscopic database. *J Quant Spectrosc Radiat Transf*. 2013;130:4-50. doi:10.1016/J.JQSRT.2013.07.002
8. Toyoda S, Yoshida N. Determination of nitrogen isotopomers of nitrous oxide on a modified isotope ratio mass spectrometer. *Anal Chem*. 1999;71:4711-4718. doi:10.1021/ac9904563
9. Brewer PJ, Kim JS, Lee S, et al. Advances in reference materials and measurement techniques for greenhouse gas atmospheric observations. *Metrologia*. 2019;56(3):1-29. doi:10.1088/1681-7575/ab1506
10. Yoshida N. ^{15}N-depleted N_2O as a product of nitrification. *Nature*. 1988;335:528-529.

doi:10.1038/335528a0

11. Kim K, Craig H. Nitrogen-15 and oxygen-18 characteristics of nitrous oxide: a global perspective. *Science*. 1993;262(5141):1855-1857. doi:10.1126/science.262.5141.1855

12. Snider DM, Venkiteswaran JJ, Schiff SL, Spoelstra J. Deciphering the oxygen isotope composition of nitrous oxide produced by nitrification. *Glob Chang Biol*. 2012;18(1):356-370. doi:10.1111/j.1365-2486.2011.02547.x

13. Rohe L, Anderson T-H, Braker G, et al. Fungal oxygen exchange between denitrification intermediates and water. *Rapid Commun Mass Spectrom*. 2014;28(4):377-384. doi:10.1002/rcm.6790

14. Richet P. *The Physical Basis of Thermodynamics With Applications to Chemistry*. 1st ed. New York: Springer Science+Business Media New York; 2001.

15. Yoshida N, Toyoda S. Constraining the atmospheric N_2O budget from intramolecular site preference in N_2O isotopomers. *Nature*. 2000;405(6784):330-334. doi:10.1038/35012558

16. Magyar PM, Orphan VJ, Eiler JM. Measurement of rare isotopologues of nitrous oxide by high-resolution multi-collector mass spectrometry. *Rapid Commun Mass Spectrom*. 2016;30(March):1923-1940. doi:10.1002/rcm.7671

17. Toyoda S, Yoshida N, Koba K. Isotopocule analysis of biologically produced nitrous oxide in various environments. *Mass Spectrom Rev*. 2017;36(2):135-160. doi:10.1002/mas.21459

18. Wang Z, Schauble EA, Eiler JM. Equilibrium thermodynamics of multiply substituted isotopologues of molecular gases. *Geochim Cosmochim Acta*. 2004;68(23):4779-4797. doi:10.1016/j.gca.2004.05.039

19. Eiler JM. "Clumped-isotope" geochemistry-The study of naturally-occurring, multiply-substituted isotopologues. *Earth Planet Sci Lett*. 2007;262(3-4):309-327. doi:10.1016/j.epsl.2007.08.020

20. Grauel AL, Schmid TW, Hu B, et al. Calibration and application of the "clumped isotope" thermometer to foraminifera for high-resolution climate reconstructions. *Geochim Cosmochim Acta*. 2013;108:125-140. doi:10.1016/j.gca.2012.12.049

21. Yeung LY. Biological signatures in clumped isotopes of O_2. *Science*. 2015;348(6233):431-434. doi:10.1126/science.aaa6284

22. Shoun H, Fushinobu S, Jiang L, Kim S-W, Wakagi T. Fungal denitrification and nitric oxide reductase cytochrome P450nor. *Philos Trans R Soc B Biol Sci*. 2012;367(1593):1186-1194. doi:10.1098/rstb.2011.0335

23. Heil J, Wolf B, Brüggemann N, et al. Site-specific ^{15}N isotopic signatures of abiotically produced N_2O. *Geochim Cosmochim Acta*. 2014;139:72-82. doi:10.1016/j.gca.2014.04.037

24. Schmidt JA, Johnson MS. Clumped isotope perturbation in tropospheric nitrous oxide from stratospheric photolysis. *Geophys Res Lett*. 2015;42(9):3546-3552. doi:10.1002/2015GL063102

25. Kaiser J, Röckmann T, Brenninkmeijer CAM. Assessment of [15]N[15]N[16]O as a tracer of stratospheric processes. *Geophys Res Lett*. 2003;30(2):16-19. doi:10.1029/2002GL016253

26. Tuzson B, Mohn J, Zeeman MJ, et al. High precision and continuous field measurements of ^{13}C and [18]O in carbon dioxide with a cryogen-free QCLAS. *Appl Phys B Lasers Opt*. 2008;92(3 SPECIAL ISSUE):451-458. doi:10.1007/s00340-008-3085-4

27. Röckmann T, Eyer S, Van Der Veen C, et al. In situ observations of the isotopic composition of methane at the Cabauw tall tower site. *Atmos Chem Phys*. 2016;16:10469-10487. doi:10.5194/acp-16-10469-2016

28. Waechter H, Mohn J, Tuzson B, Emmenegger L, Sigrist MW. Determination of N_2O isotopomers with quantum cascade laser based absorption spectroscopy. *Opt Express*. 2008;16(12):9239-9244. doi:10.1364/OE.16.00923

29. Ono S, Wang DT, Gruen DS, et al. Measurement of a doubly substituted methane isotopologue, $^{13}CH_3D$, by tunable infrared laser direct absorption spectroscopy. *Anal Chem*. 2014;86:6487-6494. doi:10.1021/ac5010579

30. Gonzalez Y, Nelson DD, Shorter JH, et al. Precise measurements of $^{12}CH_2D_2$ by tunable infrared laser direct absorption spectroscopy. *Anal Chem*. 2019;91(23):14967-14974. doi:10.1021/acs.analchem.9b03412

31. Prokhorov I, Kluge T, Janssen C. Laser absorption spectroscopy of rare and doubly substituted carbon dioxide isotopologues. *Anal Chem*. 2019;91(24):15491-15499. doi:10.1021/acs.analchem.9b03316

32. Wang Z, Nelson DD, Dettman DL, et al. Rapid and precise analysis of carbon dioxide clumped isotopic composition by tunable infrared laser differential spectroscopy. *Anal Chem*. 2020;92(2):2034-2042. doi:10.1021/acs.analchem.9b04466

33. Western CM. PGOPHER: A program for simulating rotational, vibrational and electronic spectra. *J Quant Spectrosc Radiat Transf*. 2017;186:221-242. doi:10.1016/J.JQSRT.2016.04.010

34. Toth RA. Line-frequency measurements and analysis of N_2O between 900 and 4700 cm^{-1}. *Appl Opt*. 1991;30(36):5289-5315. doi:10.1364/AO.30.005289

35. Du J, Liu A, Perevalov VI, Tashkun SA, Hu S. High-resolution infrared spectroscopy of $^{15}N_2O$ in 1650–3450 cm^{-1}. *Chinese J Chem Phys*. 2011;24(5):611-619. doi:10.1088/1674-0068/24/05/611-619

36. Wang CY, Liu AW, Perevalov VI, Tashkun SA, Song KF, Hu SM. High-resolution infrared spectroscopy of $^{14}N^{15}N^{16}O$ and $^{15}N^{14}N^{16}O$ in the 1200-3500 cm^{-1} region. *J Mol Spectrosc*. 2009;257(1):94-104. doi:10.1016/j.jms.2009.06.012

37. Jacquinet-Husson N, Armante R, Scott NA, et al. The 2015 edition of the GEISA spectroscopic database. *J Mol Spectrosc*. 2016;327:31-72. doi:10.1016/J.JMS.2016.06.007

38. Prokhorov I, Kluge T, Janssen C. Optical clumped isotope thermometry of carbon dioxide. *Sci Rep*. 2019;9:1-11. doi:10.1038/s41598-019-40750-z

39. Werner RA, Brand WA. Referencing strategies and techniques in stable isotope ratio analysis. *Rapid Commun Mass Spectrom*. 2001;15(7):501-519. doi:10.1002/rcm.258

40. Harris SJ, Liisberg J, Xia L, et al. N_2O isotopocule measurements using laser spectroscopy: analyzer characterization and intercomparison. *Atmos Meas Tech Discuss*. 2019:in review. doi:10.5194/amt-2019-451

41. Werle P, Mücke R, Slemr F. The limits of signal averaging in atmospheric trace-gas monitoring by tunable diode-laser absorption spectroscopy (TDLAS). *Appl Phys B Photophysics Laser Chem*. 1993;57(2):131-139. doi:10.1007/BF00425997

42. Griffith DWT, Parkes SD, Haverd V, Paton-Walsh C, Wilson SR. Absolute calibration of the intramolecular site preference of ^{15}N fractionation in tropospheric N_2O by FT-IR spectroscopy. *Anal Chem*. 2009;81(6):2227-2234. doi:10.1021/ac802371c

43. Flores E, Viallon J, Moussay P, Griffith DWT, Wielgosz RI. Calibration strategies for FT-IR and other isotope ratio infrared spectrometer instruments for accurate $\delta^{13}C$ and $\delta^{18}O$ measurements of CO_2 in air. *Anal Chem*. 2017;89(6):3648-3655. doi:10.1021/acs.analchem.6b05063

44. Ostrom NE, Gandhi H, Coplen TB, et al. Preliminary assessment of stable nitrogen and oxygen isotopic composition of USGS51 and USGS52 nitrous oxide reference gases and perspectives on calibration needs. *Rapid Commun Mass Spectrom*. 2018;32(15):1207-1214. doi:10.1002/rcm.8157

45. Browaeys J. Linear fit with both uncertainties in x and in y. 2019. https://www.mathworks.com/matlabcentral/fileexchange/45711-linear-fit-with-both-

uncertainties-in-x-and-in-y, retrieved December 13, 2019.

46.   Winter ERS. The decomposition of nitrous oxide on metallic oxides Part II. *J Catal*. 1970;19(1):32-40. doi:10.1016/0021-9517(70)90293-9

47.   Winter ERS. The decomposition of N_2O on oxide catalysts. *J Catal*. 1974;34:431-439. doi:10.1016/0021-9517(74)90056-6

48.   Mohn J, Gutjahr W, Toyoda S, et al. Reassessment of the NH_4NO_3 thermal decomposition technique for calibration of the N_2O isotopic composition. *Rapid Commun Mass Spectrom*. 2016;(June):2487-2496. doi:10.1002/rcm.7736

49.   Brenninkmeijer CAM, Röckmann T. Mass spectrometry of the intramolecular nitrogen isotope distribution of environmental nitrous oxide using fragment-ion analysis. *Rapid Commun Mass Spectrom*. 1999;13(20):2028-2033. doi:10.1002/(SICI)1097-0231(19991030)13:20<2028::AID-RCM751>3.0.CO;2-J

50.   Mohn J, Guggenheim C, Tuzson B, et al. A liquid nitrogen-free preconcentration unit for measurements of ambient N_2O isotopomers by QCLAS. *Atmos Meas Tech*. 2010;3(3):609-618. doi:10.5194/amt-3-609-2010

ACKNOWLEDGEMENTS

STATEMENT OF AUTHOR CONTRIBUTIONS

K.K. guided by S.M.B., L.E., and J.M. designed the study. L.Y. performed isotopic analyses using the single-laser QCLAS system. K.K. and D.Z. synthesized the doubly isotopically labelled ammonium nitrate salts; K.K. synthesized the samples of nitrous oxide from these salts. M.S.Z. and D.D.N designed and manufactured the dual-laser QCLAS instrument; B.T. supported the setup and optimization of the system at Empa and discussed the results. K.K., M.N., S.T., and N.Y. analyzed the equilibrated gases VG2, VG3, and VG4 on IRMS MAT253 Ultra at ELSI. K.K. performed the thermal equilibration experiments and calibration as well as validation experiments with QCLAS, analyzed the data and wrote the manuscript with input from all the co-authors.

ADDITIONAL INFORMATION

Competing interests: The authors declare that they have no competing interests.
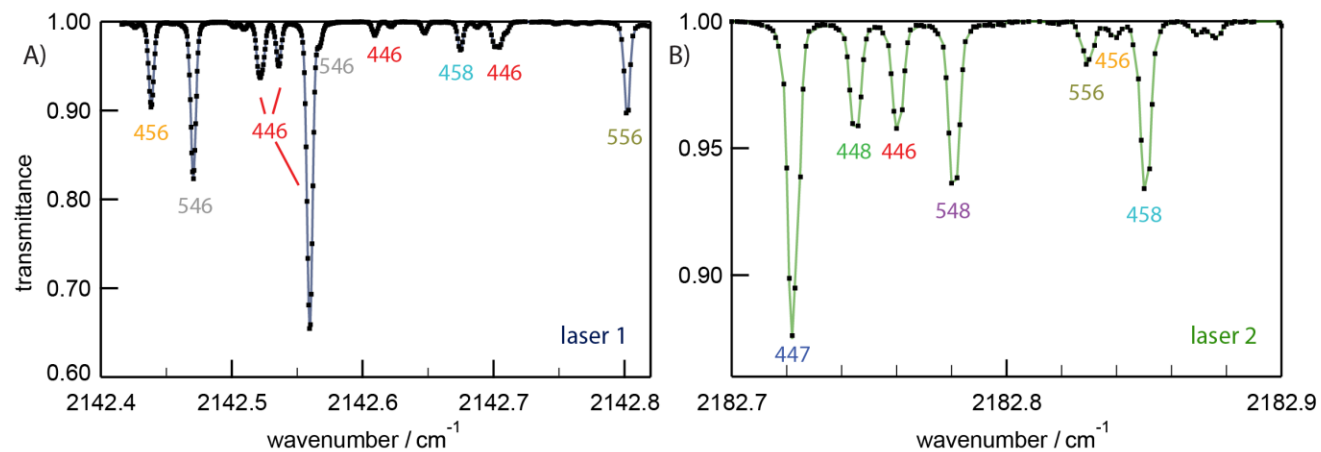
Figure 1. Measured (dots) and fitted (solid line) spectra of the N_2O isotopocules for laser 1 (A) and laser 2 (B) in QCLAS I. Spectra were measured with 1.5 % N_2O in a high-purity N_2 gas matrix.
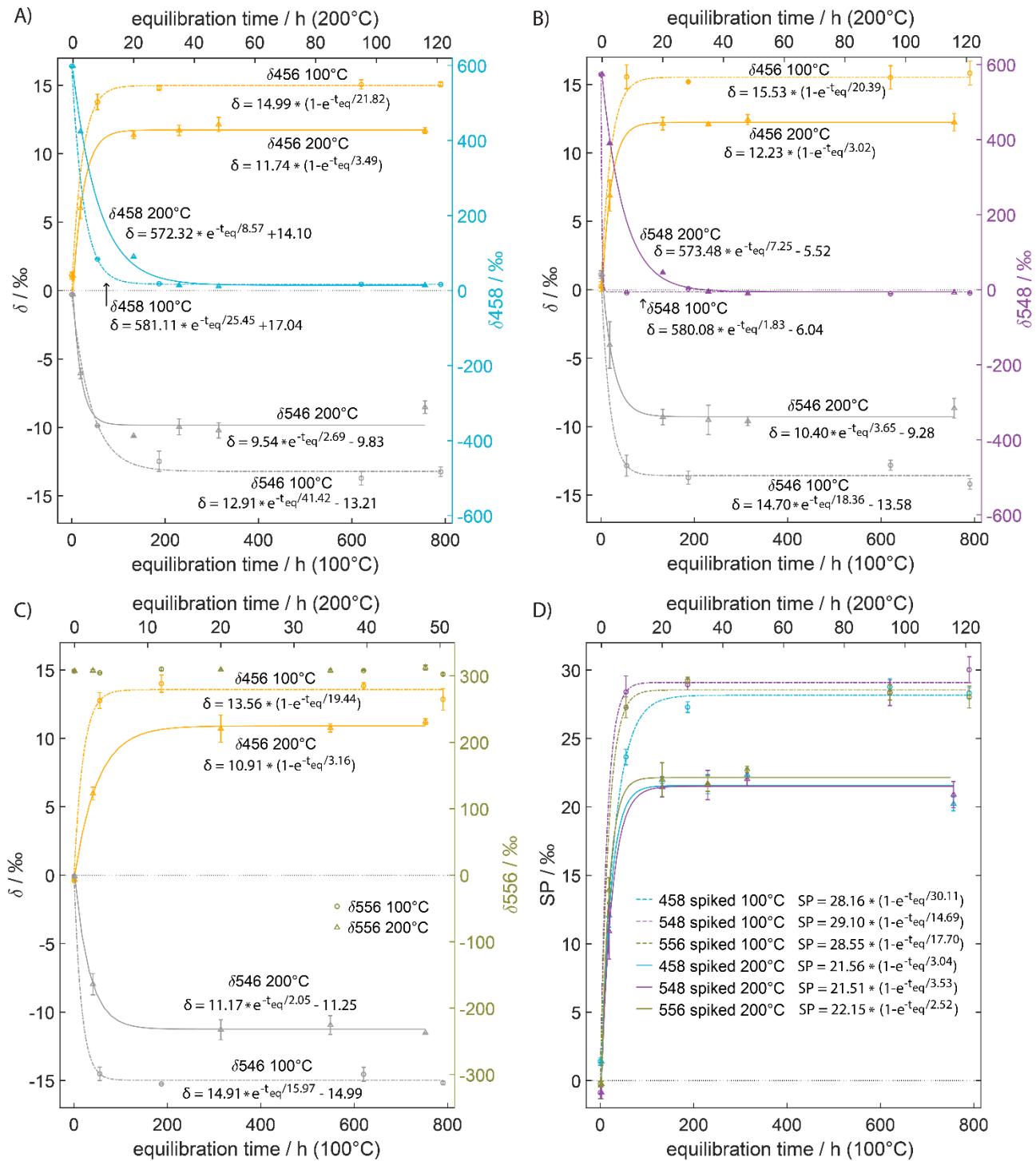
Figure 2. Progressive thermal equilibration of mixtures of N₂O with enrichment of 458 (A), 548 (B), and 556 (C) isotopocules, heated at 100 °C (dashed lines) and 200 °C (full lines) over Al₂O₃. (D) Evolution of site preference (SP) in N₂O mixtures during thermal equilibration at 100 °C (dashed lines) and 200 °C (full lines). The data is fitted using exponential decay and saturation functions.
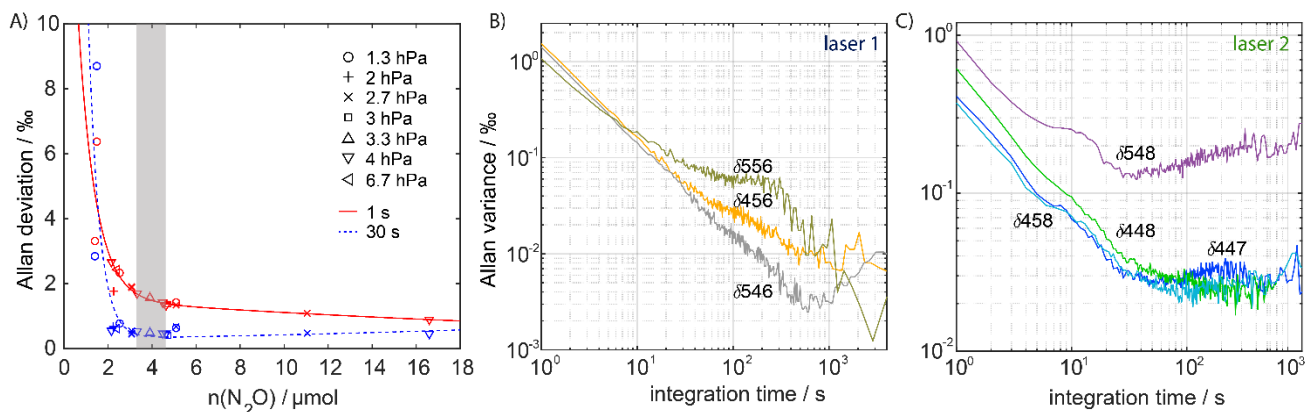
Figure 3. Allan variance plots. (A) δ^{548} ($^{15}N^{14}N^{18}O$) as a function of N_2O molar amount in the multipass cell for 1 s (red, solid line) and 30 s (blue, dashed line) spectral averaging. The grey-shaded area indicates the range of N_2O molar amounts yielding optimal measurement precision expressed as Allan deviation (3 – 4 µmol). (B, C) Allan variance of δ values of all N_2O isotopocules measured by the QCLAS I.
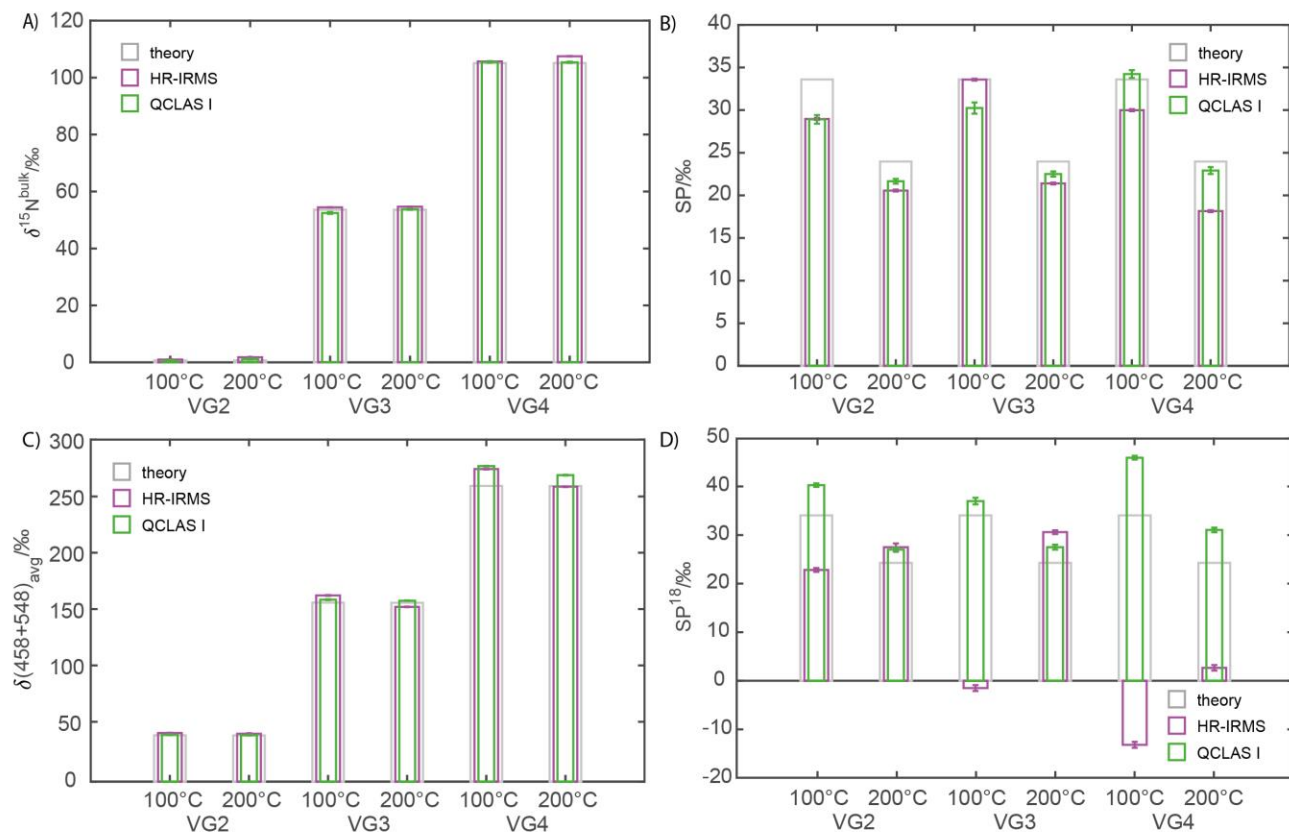
Figure 4. Comparison of theoretically predicted isotopic values (wide, grey columns) of equilibrated validation gases with experimental values from QCLAS I (narrow, green columns) and HR-IRMS (magenta columns).

Table 1. Site-specific isotopic composition of N_2O gases spiked with clumped isotopocules and equilibrated at 100 and 200 °C over Al_2O_3. In comparison to results from Magyar et al.[16] and values derived from theoretical statistical thermodynamics by Wang et al.[18]

temperature / °C	spike	SP / ‰ QCLAS I	SP / ‰ QCLAS II	SP / ‰ HR-IRMS[16]	SP / ‰ theory	SP[18] / ‰ QCLAS I	SP[18] / ‰ theory[18]
100 °C	458	28.70±0.39	28.94±0.16			26.25±0.58	
	548	28.33±0.38	29.11±0.22	34.19±0.43	33.75	26.48±0.37	34.06
	556	28.65±0.23	30.00±0.17			27.53±0.53	
200 °C	458	21.76±0.42	21.77±0.09			20.31±0.54	
	548	21.60±0.49	23.53±0.19	23.28±0.43	24.07	21.74±0.54	24.27
	556	22.75±0.22	22.42±0.12			22.04±0.38	

Table 2: Experimental results to validate QCLAS results applying the mole fraction calibration scheme. First, results for VG1 by QCLAS I were compared to QCLAS II and IRMS using conventional δ-calibration. Second, for VG2, VG3, and VG4 equilibrated at 200 °C, theoretically predicted δ and Δ values were compared to experimental δ and Δ values analyzed by QCLAS I and IRMS MAT253 Ultra (HR-IRMS). Given uncertainty: QCLAS I – repeatability for multiple sample measurement sequences (VG1: N = 15, five triplicates; VG2, VG3, VG4: N = 5); QCLAS II – repeatability for multiple sample measurement sequence (N = 12, three quadruplicates); IRMS: fully propagated standard error of a sample; HR IRMS – repeatability for one measurement sequence (N = 6).
[*] deviation due to limited span of available standards for $\delta^{18}O$
[†] correction described in the main text

	δ456 / ‰	δ546 / ‰	δ447 / ‰	δ448 / ‰	Δ556 / ‰	Δ(458+548)$_{avg}$ / ‰	SP^{18} / ‰
VG1							
QCLAS I	15.53±0.16	16.27±0.17	21.41±0.09	55.13±0.24	0.68±0.65	−0.66±0.14	4.70±0.09
QCLAS II	15.82±0.06	16.80±0.08	-	53.93±0.06[*]	-	-	-
IRMS	-	-	-	55.96±0.07	-	-	-
VG2							
QCLAS I	−1.75±0.20	−0.62±0.31	21.28±0.18	40.46±0.52	0.95±0.66	0.86±0.55	3.26±0.59
QCLAS II	0.30±0.20	1.05±0.38	-	38.90±0.36[*]	-	-	-
IRMS	-	-	-	39.79±0.07	-	-	-
VG2 equilibrated at 200 °C							
theory	12.74	−11.32	20.54	39.78	0.12	0.12	24.26
QCLAS I	11.98±0.19	−9.77±0.20	21.86±0.15	40.69±0.21	−1.49±0.64	−0.77±0.25	27.00±0.44
HR-IRMS	12.08±0.06	−8.56±0.10	20.84±0.03	41.32±0.01	-	−0.96±0.40[†]	27.49±0.79[†]
VG3							
QCLAS I	52.54±0.28	55.89±0.18	24.60±0.24	105.96±0.27	7.60±1.53	1.40±0.72	1.96±0.22
QCLAS II	51.02±0.16	54.99±0.06	-	99.68±0.34[*]	-	-	-
IRMS	-	-	-	104.14±0.07	-	-	-
VG3 equilibrated at 200 °C							
theory	65.11	41.05	24.49	104.14	0.12	0.12	24.26
QCLAS I	64.54±0.26	41.93±0.16	26.17±0.30	102.35±0.34	7.65±0.59	3.76±0.37	27.50±0.50
HR-IRMS	64.87±0.06	43.38±0.10	24.41±0.02	100.05±0.01	-	−0.46±0.20[†]	30.59±0.37[†]
VG4							
QCLAS I	101.23±0.34	100.22±0.85	29.39±0.17	157.22±0.09	24.54±1.33	8.03±0.90	5.17±0.11
QCLAS II	102.71±0.16	104.93±0.50	-	148.02±0.70[*]	-	-	-
IRMS	-	-	-	155.86±0.14	-	-	-
VG4 equilibrated at 200 °C							
theory	116.11	92.04	27.63	155.86	0.12	0.12	24.26
QCLAS I	115.87±0.40	92.86±0.05	29.95±0.15	152.02±0.28	21.83±0.63	13.44±0.42	31.05±0.49
HR-IRMS	115.59±0.05	97.36±0.10	28.16±0.09	149.22±0.18	-	3.74±0.31[†]	2.67±0.56[†]